Classical and Quantum Magnetic Phenomena in Natural and Artificial Ferritin Proteins

S. Gider, D. D. Awschalom,* T. Douglas, S. Mann, M. Chaparala

Artificial ferritin has been synthesized with control of both the magnetic state (antiferromagnetic or ferrimagnetic) and the particle size over an order of magnitude in the number of iron atoms. The magnetic properties of the artificial ferritin were compared with those of natural horse spleen ferritin in a range of temperatures (20 millikelvin to 300 kelvin) and fields (1 nanotesla to 27 tesla). In the classical regime, the blocking temperature was found to correlate with the average particle size. A correlation was also observed in the quantum regime between the resonance frequency of macroscopic quantum tunneling of the Néel vector and the particle size. At high magnetic fields (to 27 tesla), a spin flop transition with a strong dependence on orientation was seen in the natural ferritin, providing evidence of antiferromagnetism in this system.

The iron-protein complex ferritin consists of a central core of hydrated Fe(III) oxide encapsulated within a multisubunit protein shell. The dimensions of the polypeptide cavity establish an 8-nm limit on the diameter of the mineral core, which is synthesized in situ within intact protein molecules. This protein is of interest to researchers in a range of fields: In the biology of mammals and bacteria, ferritin serves as the main form of Fe storage (*1*, *2*); in the chemical synthesis of organic-inorganic nanostructures, the protein shell (apoferritin) can serve as a host for inorganic materials (*3*–*5*); and in the physics of magnetism, ferritin is one of the smallest realizable magnets and displays a variety of classical and quantum spin phenomena (*6*, *7*).

Despite extensive studies on horse spleen ferritin, fundamental issues remain unresolved. With a large surface to volume ratio, the properties of ferritin must be strongly dependent on the size of the proteins, but the size of available samples is determined largely by natural processes. Discussions of the magnetic behavior of ferritin usually begin with the assumption of an antiferromagnetic spin arrangement, but the evidence for antiferromagnetism is indirect (*8*, *9*). Recent progress in the synthesis of Fe compounds within demetallated ferritin (apoferritin) indicate that it is possible to control the extent of Fe loading within the Fe cavity (*10*) and the magnetic state (antiferromagnetic or ferrimagnetic) of the mineral core (*4*). This makes possible a more systematic study of the magnetic properties of these nanometer-scale proteins. Knowledge gained by magnetic studies can in turn lead to better understanding of the chemical synthesis process and ultimately to the elucidation of the biological function of the natural proteins.

To this end, we synthesized a series of artificial ferritin samples beginning with the empty apoferritin shell. In what we call the "magnetoferritin" sample a ferrimagnetic core was synthesized, and in the other samples the same antiferromagnetic material, which constitutes the natural ferritin core, was synthesized with metal loading values from 100 to 4000 Fe ions. Measurements of the classical magnetic properties at temperatures from 5 to 300 K and fields up to 5 T revealed a correlation between the mean particle size and the blocking temperature. At lower temperatures (20 to 200 mK) and fields (~1 nT), the quantum spin dynamics of the antiferromagnetic ferritin shows a correlation between mean particle size and the tunneling rate; specifically, the mean particle size scales with the logarithm of the resonance frequency for macroscopic quantum tunneling of the Néel vector, as predicted by theory (*11*, *12*). Finally, we performed measurements at high magnetic fields (to 27 T) to study the saturation of the magnetic moment and anisotropy of the ferritin films. A spin flop transition was observed, providing additional evidence of antiferromagnetism in ferritin.

We synthesized a series of artificial ferritin samples by chemical reconstitution of iron oxide cores within the empty polypeptide shell of apoferritin. The magnetoferritin sample, consisting of a ferrimagnetic core of magnetite-maghemite (Fe_3O_4–γ-Fe_2O_3), was synthesized by an extension of earlier methods (*4*). In other experiments, an antiferromagnetic material, ferrihydrite ($5Fe_2O_3 \cdot 9H_2O$), which constitutes the core of natural ferritin, was synthesized within the protein shell with metal loading values from 100 to 4000 Fe ions per ferritin molecule. Apoferritin was prepared by thioglycolic reduction of horse spleen ferritin (*13*) and remineralized by the air oxidation of a solution of $NH_4Fe(SO_4)_2$ added in aliquots to the protein solution at pH 6.5 in 0.1 M MOPS buffer to give the required metal:protein loading (*14*). The samples were characterized by chemical and biochemical analysis and transmission electron microscopy (TEM) (Table 1).

Natural horse spleen ferritin is widely believed to become antiferromagnetic at 240 K (*8*, *9*). However, the evidence is largely indirect because the particles are superparamagnetic and, as a result, the magnetization is substantially reduced at high temperatures and cannot be followed through the Néel point. At lower temperatures (10 to 50 K), there is not enough thermal energy to allow the moments to oscillate across the magnetic anisotropy barrier, and they become blocked.

Although Mössbauer spectroscopy is the traditional technique for the study of magnetism in ferritin, it is necessary to extract the bulk magnetic properties from Mössbauer data by fitting to a model. A superconducting quantum interference device (SQUID) directly probes the bulk properties on a larger length and time scale. Initial magnetic studies were done at temperatures ranging from 2 to 300 K and fields up to 5 T in a radio-frequency SQUID magnetometer. The magnetoferritin sample consisted of 0.16 mg of protein, and the artificial antiferromagnetic samples consisted of 0.25 mg each. The magnetic properties of a sample of natural horse spleen ferritin (0.4 mg) from a commercial solution (*15*) were also measured for comparison. Before measuring, the artificial samples were dried in air at 40°C on a 25-μm-thick polypropylene film, and the natural samples were dried at room temperature on a glass slide.

A marked contrast between the magnetoferritin and the natural ferritin can be seen in the variation of magnetization with

Table 1. Characteristics of the natural and artificial ferritin samples used in the present study.

Sample*	Diameter† (nm)	
	Mean	Variance
Natural ferritin	5–6	
Magnetoferritin	7.3	1.4
100	2.1‡	
250	2.8‡	
500	3.9	1.0
1000	4.4	0.8
2000	5.6	0.7
3000	6.4	0.6
4000	6.4	0.9

*Iron content was measured by atomic absorption analysis and the Lowry method. †Particle sizes determined by TEM. ‡TEM gives an upper limit of 3 nm. We obtained the diameters shown by assuming a linear relation between volume and the number of Fe ions.

S. Gider and D. D. Awschalom, Department of Physics, University of California, Santa Barbara, CA 93106, USA.
T. Douglas and S. Mann, School of Chemistry, University of Bath, Bath BA2 7AY, UK.
M. Chaparala, National High Magnetic Field Laboratory, Tallahassee, FL 32306, USA.
*To whom correspondence should be addressed.

field at low temperatures (Fig. 1A). At the highest field, the moment of the magnetoferritin is over 10 times that of the natural ferritin, which is consistent with the identification by x-ray analysis of the magnetoferritin as either magnetite or maghemite, both ferrimagnetic compounds. Together with the absence of hysteresis, the sharp reversal in magnetization indicates that the anisotropy of the magnetoferritin must be weak. In contrast, natural ferritin displays a slight hysteresis and remanence that disappear when the temperature is raised to 30 K. Thus, above a certain temperature, the anisotropy barrier is overcome by thermal fluctuations, leading to classical superparamagnetic behavior.

In reality, there is a distribution of anisotropy barriers due to the distribution in particle sizes. Even if the magnetic anisotropy K does not vary from particle to particle, there will be variations in the volume V because of variations in particle size and hence a distribution of energy barriers KV. A system with a distribution of energy barriers will often display glassy behavior. In a spin glass, the distribution arises from frustrated interparticle exchange interactions and disorder. In ferritin, however, the distribution is due to intraparticle variations in anisotropy energy barriers. This can be seen in Fig. 1, B and C. The pair of curves that merge (filled and open circles) were taken while warming in the presence of a 50-G field: for the field-cooled (FC) curve, the sample was cooled beforehand from room temperature to 5 K in a 50-G field, thereby annealing the spins into stable states; for the zero field-cooled (ZFC) curve, the sample was cooled in a low field (<2 G) from room temperature to 5 K, allowing the spins to relax into metastable states, and then the 50-G field was applied at 5 K. Two competing effects are responsible for the appearance of a peak in the ZFC curves at the mean blocking temperature T_B: As the temperature is raised, the blocked spins are activated. This activation produces an increase in the magnetization whereas unblocked spins suffer more thermal fluctuations, leading to a decrease in the magnetization.

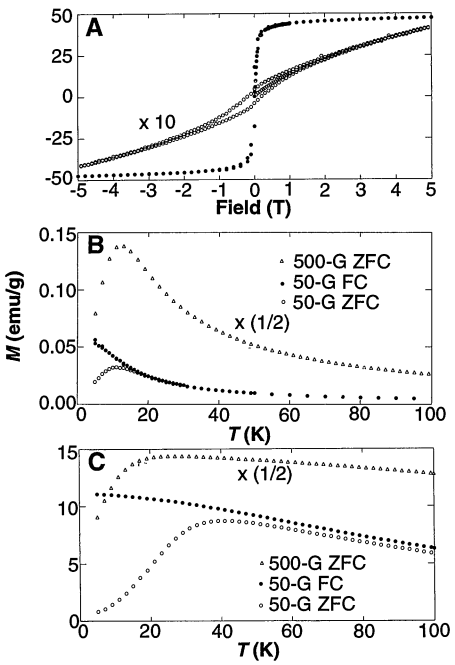

Fig. 1. (**A**) Magnetization versus field (at 5 K) for ferrimagnetic artificial ferritin ("magnetoferritin") (filled circles) and natural horse spleen ferritin (open circles). (**B** and **C**) Variation in magnetization versus temperature after cooling in a field (FC sample) and cooling in zero field (ZFC sample) for the natural horse spleen ferritin (B) and the magnetoferritin (C). The mass includes the apoferritin as well as the iron oxide core; emu, electromagnetic unit.

Although the difference between the FC and ZFC curves in natural ferritin has been observed in a single field, the interpretation was not in terms of glassy behavior (*16*). Our interpretation follows more closely that proposed as a result of work on other small ferro- and ferrimagnetic particles (*17*, *18*). In the present study, a comparison was made between antiferromagnetic (Fig. 1B) and ferrimagnetic (Fig. 1C) particles. In contrast to the case in the field sweep (Fig. 1A), anisotropy can be observed in the temperature sweep (Fig. 1C) on magnetoferritin through the difference in the FC and ZFC curves. The FC and ZFC curves of natural ferritin become indistinguishable by 20 K (Fig. 1B). Because the magnetization increases rapidly with field for the magnetoferritin (Fig. 1A), a small difference (0.5%) in the field set for the FC and ZFC curves (Fig. 1C) produces an offset (they would otherwise merge around 50 K). Accordingly, T_B is higher in the magnetoferritin than in natural ferritin, 40 K versus 11 K, respectively, suggesting a higher anisotropy barrier KV. The anisotropy of the magnetoferritin is not seen in the field sweep because of the suppression of the barrier with application of a field. An increase of the field from 50 to 500 G decreases T_B to 25 K in the magnetoferritin, whereas in natural ferritin there is only a slight shift to higher temperatures. The reduction of T_B with increasing field has been observed in other small ferrimagnetic systems (*18*), but there does not appear to be any observation of the opposite effect in antiferromagnetic systems. Dipolar interactions between particles appear to be insignificant at these temperatures, as T_B does not vary upon dilution of the natural ferritin with apoferritin to one-hundredth of its concentration (to a concentration comparable to that of the artificial ferritin). A more likely possibility is that shape anisotropy is less important for the antiferromagnetic samples than for the ferrimagnetic ones (*9*) because of the smaller moment per particle of the former [~300 Bohr magnetons (μ_B) per particle] versus the latter (~10,000 μ_B per particle).

The glassy behavior of ferritin can also be studied as a function of particle size. A range of antiferromagnetic samples with Fe loading from 100 to 4000 were examined under FC and ZFC conditions (Fig. 2A). As with natural ferritin, the FC curves (not shown) merged with the ZFC curves at temperatures by 30 K. In addition, T_B decreased with decreasing particle size (Fig. 2A). The peak in the ZFC curve does not occur exactly at T_B; rather, the peak is proportional to T_B by a factor that depends on the form of the distribution of the particle sizes. This factor can range from 1 for a delta function distribution to 2 for a uniform distribution (*17*). A reasonable assumption is that the form of the distribution is the same for all of the samples. If the anisotropy constant also does not vary from particle to particle, then T_B should scale linearly with the volume of the particles, as seen in Fig. 2B.

Another study (*19*) of the variation of T_B with particle size over a smaller range (Fe loading of 1000 to 2000) found a nonlinear component in the dependence due to a surface anisotropy. The samples in this

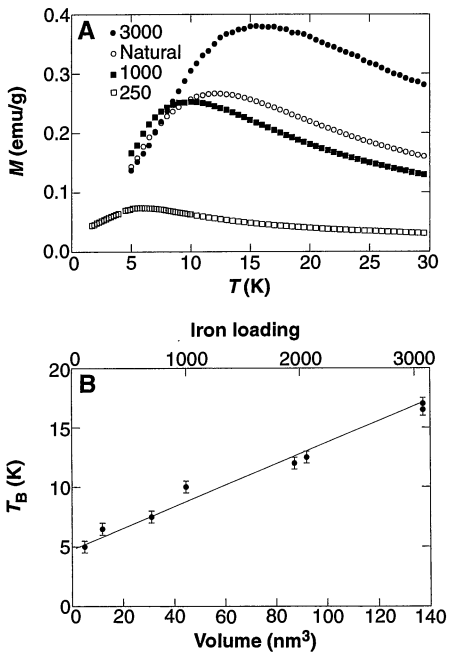

Fig. 2. (**A**) Variation in magnetization for different particle sizes upon warming in a field of 500 G after cooling in zero field. The peak in the curves is the mean blocking temperature, T_B. (**B**) Dependence of T_B on mean particle size. The sample with an Fe loading of 4000 was found by TEM measurements (see Table 1) to have the same mean diameter as the sample with an Fe loading of 3000 and hence the same T_B.

study (*19*) were prepared by reduction of natural horse spleen ferritin, whereas ours were prepared by oxidation in the empty apoferritin. A difference in the surfaces could give a larger contribution to the anisotropy from surface spins in the reduced case. The T_B values measured in this study are consistently higher than in the present study because of the difference in the time scale of the measurements. Unblocking occurs when the moments fluctuate on a time scale that is short as compared to the measurement. Because the intrinsic Mössbauer time scale is the nuclear Larmor precession (nanoseconds) whereas the radio-frequency SQUID time scale is the scanning of the sample through the detection coils (seconds), the T_B values obtained from the Mössbauer studies will be higher. For smaller particles, the relation between T_B and V must become more complex and cannot simply be linearly extrapolated from the data in Fig. 2B.

Experiments at lower temperatures and fields provide further evidence that the magnetic properties of the artificial ferritin reconstituted with ferrihydrite cores are determined more by particle size than by variations in anisotropy. At temperatures far below T_B, the net magnetization is classically forbidden from fluctuating to the opposite direction because there is not enough thermal energy to overcome the anisotropy barrier. The net magnetization, described in terms of the Néel vector, may nevertheless coherently tunnel quantum mechanically across the barrier. This effect is observed as a resonance in the frequency-dependent magnetic susceptibility and has been observed in natural horse spleen ferritin (*7*, *20*).

Similar studies of the artificial ferritin were undertaken to complement the studies of the classical magnetic properties and to test the predictions of theories of macroscopic quantum tunneling (MQT). The experimental technique has been described (*20*): an integrated dc SQUID magnetometer is used to study the spin dynamics of the artificial antiferromagnetic ferritin by making measurements of magnetic noise and susceptibility at temperatures from 20 to 200 mK and fields on the order of a nanotesla. A typical noise resonance curve is shown in the inset of Fig. 3. Qualitatively, as the particle size becomes smaller and the anisotropy is reduced, the Néel vector will tunnel across the barrier at a higher rate. The resonance frequency should thus increase as the particle size decreases. The theory of MQT in antiferromagnets (*11*, *12*) predicts that the resonance frequency ν_{res} should depend on the size of the particle V in the form

$$\nu_{res} = \nu_0 \exp\left(-\frac{V}{\mu_B}\sqrt{\chi_\perp K}\right) \quad (1)$$

where ν_0 is the attempt frequency, $\chi_\perp$ is the transverse susceptibility, and K is the anisotropy along the easy axis for magnetization. The dependence on the volume V can be written explicitly as

$$\ln\left(\frac{\nu_{res}}{\nu_0}\right) \approx -\frac{V_0}{\mu_B}\sqrt{\chi_\perp K}\left(\frac{V}{V_0}\right) \quad (2)$$

where V_0 can be taken to be the volume of natural ferritin. A graph of the logarithm of ν_{res} versus V/V_0 (Fig. 3) shows good agreement with the predicted linear scaling behavior. The volumes are normalized by the volume in the natural horse spleen ferritin, which has 4500 Fe(III) spins. The sample of natural horse spleen ferritin that we used in the study of quantum magnetic phenomena was extracted by ultracentrifuge from the commercial solution with the selection criterion being those particles of largest size. Hence, the upper tail of the distribution of particles was chosen instead of the whole distribution as in the study of the classical magnetic phenomena. The data of Fig. 3 demonstrate that the resonance effects originate from the magnetic core of the ferritin, not from an alternative source, and are consistent with the theory of magnetic MQT (*20*, *21*). On the basis of both classical and quantum phenomena, we may conclude that the magnetic properties of natural and artificial ferritin scale with particle size.

The behavior of ferritin at high magnetic fields (>20 T) is a previously unexplored regime but one that can reveal valuable information about the exchange interactions. There was an early report (*22*) of a metamagnetic transition at 7.5 T in experiments with pulsed fields up to 17.5 T, but this transition could not be confirmed (*23*). In our work we studied natural horse spleen ferritin and artificial antiferromagnetic ferritin at temperatures from 2 to 30 K and static fields up to 27 T with a highly sensitive cantilever magnetometer (*24*). A marked difference can be seen in Fig. 4 in natural horse spleen ferritin when the field is parallel and when it is perpendicular to the plane of the dried ferritin film, in marked contrast to the assumption that a bulk ferritin sample is essentially a powder. The direction parallel to the thin self-supporting film of ferritin appears to be an easy axis for magnetization, most likely due to strain-induced anisotropy during drying.

The sensitivity of the transition at 10.7 T to the orientation is evidence for its identification as a spin flop transition, which is a direct indication of antiferromagnetism in ferritin. At 30 K, when the anisotropy barrier is small compared to thermal fluctuations, no transition is observed. The critical field for a spin flop transition in a bulk crystal is to lowest order given by (*25*)

$$H_c = \sqrt{R2H_eH_a - H_a^2} \quad (3)$$

where H_e is the exchange field and H_a is the anisotropy field. Recent Mössbauer spectroscopy of ferritin at fields up to 14 T (*26*) allows values of H_e and H_a to be extracted, specifically 130 T and 1.72 T, respectively, which implies a bulk spin flop at 21.1 T. The observation of a nonhysteretic transition at 10.7 T and the fact that the linear segment that follows the transition does not extrapolate to zero magnetization at zero field suggest that the transition is not one in the bulk but only on the surface (*27*). Given the large surface/volume ratio of the ferritin, the surface spins are likely to have a significant, but different, role than the bulk spins because they can experience different exchange and anisotropy fields. We

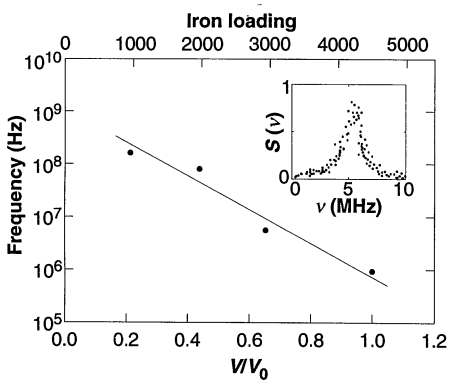

Fig. 3. Dependence of resonance frequency, ν_{res}, on particle size, V/V_0. Note that frequency is plotted on a logarithmic scale in accord with quantum mechanical predictions. The inset shows a typical noise resonance curve $S(\nu)$ observed for the sample with an Fe loading of 3000 at 24.3 mK in a background field of ~1 nT.

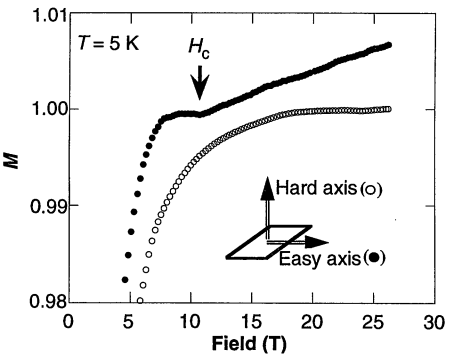

Fig. 4. Relative magnetization of natural horse spleen ferritin at high fields. For the easy axis curve the plane of the ferritin film is oriented parallel to the magnetic field, and for the hard axis curve the plane is perpendicular to the field. The easy axis curve is normalized to its value just before the transition, and the hard axis curve is normalized to its saturation value at maximum field. The downward-pointing arrow indicates the critical field (H_c) for the spin flop transition. The effects are antisymmetric with reversal of the field.

also studied one of the artificial samples (the one with an Fe loading of 1000) in the perpendicular orientation, and no transition was seen at 5 K up to 15 T. Additional experiments with artificial samples of different particle sizes should provide a better understanding of the effects due to the surface spins.

The fabrication of small magnets in a biological host through chemical synthesis presents the opportunity to study nanometer-scale magnetism with a systematic variation of interactions and particle size. Both in the classical regime of intermediate fields and temperatures and in the quantum regime of low fields and temperatures, correlations are found between the particle size and the magnetic properties of the artificial ferritin consistent with the properties of natural ferritin. In another classical regime of high magnetic fields, the anisotropy of the ferritin films is found to be crucial in competition with the antiferromagnetic exchange to produce the spin flop transition. Complementary measurements on the transition such as antiferromagnetic resonance and specific heat would also be desirable.

The ferritin protein is of interest not only in pure research but in applied technologies as well. In addition to serving as a vesicle for the chemical fabrication of new materials, the ferritin protein could also serve as a biomagnetic coating for imaging structural defects in ferrous materials (*28*). There has also been recent work on the use of other superparamagnetic particles as a refrigerant (*29*). Other applications closer to the original source of ferritin include the enhancement of magnetic resonance images in biological studies (*30*) and in the orientation of biological assemblies (*31*). All of these research and practical applications require specific knowledge of the synthesis and spin interactions of biomagnetic entities.

REFERENCES AND NOTES

1. G. C. Ford *et al.*, *Philos. Trans. R. Soc. London Ser. B* **304**, 551 (1984).
2. P. M. Harrison and T. G. Hoy, in *Inorganic Biochemistry*, G. L. Eichhorn, Ed. (Elsevier, Amsterdam, 1973), vol. 1, p. 253.
3. F. C. Meldrum, V. J. Wade, D. L. Nimmo, B. R. Heywood, S. Mann, *Nature* **349**, 684 (1991).
4. F. C. Meldrum, B. R. Heywood, S. Mann, *Science* **257**, 522 (1992). Initial magnetic measurements on magnetoferritin were reported in J. W. M. Bulte *et al.*, *Invest. Radiol.* **29**, S214 (1994).
5. P. Mackle, J. M. Charnock, C. D. Garner, F. C. Meldrum, S. Mann, *J. Am. Chem. Soc.* **115**, 8471 (1993).
6. T. G. St. Pierre, J. Webb, S. Mann, in *Biomineralization: Chemical and Biochemical Perspectives*, S. Mann, J. Webb, R. J. P. Williams, Eds. (VCH, Weinheim, Germany, 1989), p. 295.
7. D. D. Awschalom, D. P. DiVincenzo, J. F. Smyth, *Science* **258**, 414 (1992).
8. E. R. Bauminger and I. Nowik, *Hyperfine Interactions* **50**, 489 (1989).
9. S. H. Bell *et al.*, *Biochim. Biophys. Acta* **787**, 227 (1984).
10. S. Mann, J. M. Williams, A. Treffry, P. M. Harrison, *J. Mol. Biol.* **198**, 405 (1987).
11. B. Barbara and E. M. Chudnovsky, *Phys. Lett. A* **145**, 205 (1990).
12. I. V. Krive and O. B. Zaslavskii, *J. Phys. Condens. Matter* **2**, 9457 (1990).
13. A. Treffry and P. Harrison, *Biochem. J.* **171**, 313 (1978).
14. I. G. Macara, T. G. Hoy, P. M. Harrison, *ibid.* **126**, 151 (1972).
15. Obtained from Sigma Chemical Company, St. Louis, MO 63178.
16. J. Tejada and X. X. Zhang, *J. Phys. Condens. Matter* **6**, 263 (1994).
17. J. I. Gittelmann, B. Abeles, S. Bozowski, *Phys. Rev. B* **9**, 3891 (1974).
18. R. W. Chantrell, M. El-Hilo, K. O'Grady, *IEEE Trans. Magn.* **27**, 3570 (1991).
19. R. B. Frankel, G. C. Papaefthymiou, G. D. Watt, *Hyperfine Interactions* **66**, 71 (1991).
20. D. D. Awschalom, J. F. Smyth, G. Grinstein, D. P. DiVincenzo, D. Loss, *Phys. Rev. Lett.* **68**, 3092 (1992).
21. D. D. Awschalom, D. P. DiVincenzo, G. Grinstein, D. Loss, *ibid.* **71**, 4276 (1993).
22. J. L. Girardet *et al.*, *J. Appl. Phys.* **41**, 1002 (1970).
23. A. Blaise and J. L. Girardet, in *International Conference of Magnetism* (Nauka, Moscow, 1973), p. 280.
24. M. Chaparala, O. H. Chung, M. J. Naughton, in *AIP Conference Proceedings 273: Superconductivity and Its Applications* (Buffalo, NY, 1992), H. S. Kwok, D. T. Shaw, M. J. Naughton, Eds. (American Institute of Physics, New York, 1992), p. 407.
25. F. Keffer, in *Handbuch der Physik: Ferromagnetism*, H. P. J. Wijn, Ed. (Springer-Verlag, Berlin, 1966), vol. XVIII/2, p. 134.
26. C. Hunt, Q. A. Pankhurst, D. P. E. Dickson, *Hyperfine Interactions*, **91**, 821 (1994).
27. D. L. Mills, *Phys. Rev. Lett.* **20**, 18 (1968); F. Keffer and H. Chow, *ibid.* **31**, 1061 (1973).
28. Q. A. Pankhurst and R. J. Pollard, *J. Phys. Condens. Matter* **5**, 8487 (1993).
29. R. F. Service, *Science* **264**, 510 (1994).
30. S. Cerdan, H. R. Lotscher, B. Kunnecke, J. Seelig, *Magn. Reson. Med.* **12**, 151 (1989).
31. S. W. Charles, *J. Magn. Magn. Mater.* **85**, 277 (1990).

32. This work was supported by Air Force Office of Scientific Research grant F49620-93-1-0117. This work also made use of the University of California at Santa Barbara Materials Research Laboratory Central Facilities supported by the National Science Foundation (NSF) under award DMR-9123048. A portion of this work was performed at the National High Magnetic Field Laboratory, Tallahassee, which is supported by NSF cooperative agreement DMR-9016241 and by the State of Florida. We have also benefited from helpful discussions with D. DiVincenzo and G. Grinstein.

6 October 1994; accepted 6 February 1995

E5531, a Pure Endotoxin Antagonist of High Potency

William J. Christ, Osamu Asano, Andrea L. C. Robidoux, Michel Perez, Yuan Wang, Gloria R. Dubuc, Wendy E. Gavin, Lynn D. Hawkins, Pamela D. McGuinness, Maureen A. Mullarkey, Michael D. Lewis, Yoshito Kishi,*† Tsutomu Kawata, John R. Bristol, Jeffrey R. Rose, Daniel P. Rossignol, Seiichi Kobayashi, Ieharu Hishinuma, Akifumi Kimura, Naoki Asakawa, Kouichi Katayama, Isao Yamatsu*

Shock due to Gram-negative bacterial sepsis is a consequence of acute inflammatory response to lipopolysaccharide (LPS) or endotoxin released from bacteria. LPS is a major constituent of the outer membrane of Gram-negative bacteria, and its terminal disaccharide phospholipid (lipid A) portion contains the key structural features responsible for toxic activity. Based on the proposed structure of nontoxic *Rhodobacter capsulatus* lipid A, a fully stabilized endotoxin antagonist E5531 has been synthesized. In vitro, E5531 demonstrated potent antagonism of LPS-mediated cellular activation in a variety of systems. In vivo, E5531 protected mice from LPS-induced lethality and, in cooperation with an antibiotic, protected mice from a lethal infection of viable *Escherichia coli*.

Despite the availability of an array of potent antibiotics, shock due to Gram-negative bacterial sepsis remains a serious unsolved clinical problem (*1*). It is probable that the antimicrobial, cytolytic properties of antibiotics induce the release of LPS from the outer membrane of Gram-negative bacteria (*2*). In humans, acute inflammatory responses to LPS or lipid A (Fig. 1) or both (*3*) result in the release of cytokines and other cellular mediators, including tumor necrosis factor–α (TNF-α), interleukin-1 (IL-1), IL-6, leukotrienes, and thromboxane A2 from monocytes and macrophages (*4*). At extreme levels, these cytokines and cellular mediators are known to

W. J. Christ, O. Asano, A. L. C. Robidoux, M. Perez, Y. Wang, G. R. Dubuc, W. E. Gavin, L. D. Hawkins, P. D. McGuinness, M. A. Mullarkey, M. D. Lewis, Y. Kishi, T. Kawata, J. R. Bristol, J. R. Rose, D. P. Rossignol, Eisai Research Institute, Andover, MA 01810–2441, USA.
S. Kobayashi, I. Hishinuma, A. Kimura, N. Asakawa, K. Katayama, I. Yamatsu, Tsukuba Research Laboratories, Eisai Co., Tsukuba, Ibaraki, JAPAN.

*To whom correspondence should be addressed.
†Participated in the capacity of the Chairman of Advisory Board.